

Isoform Composition of Connexin Channels Determines Selectivity among Second Messengers and Uncharged Molecules*

(Received for publication, June 25, 1997, and in revised form, November 3, 1997)

Carville G. Bevans‡, Marianne Kordel§¶, Seung K. Rhee||, and Andrew L. Harris‡**

From the ‡Thomas C. Jenkins Department of Biophysics, Johns Hopkins University, Baltimore, Maryland 21218, the §Department of Enzyme Technology, Gesellschaft für Biotechnologische Forschung, Mascheroder Weg 1, 38124 Braunschweig, Germany, and the ||Department of Biochemistry, Yeungnam University, 214-1 Daedong, Kyoungsan, Republic of Korea

Intercellular connexin channels (gap junction channels) have long been thought to mediate molecular signaling between cells, but the nature of the signaling has been unclear. This study shows that connexin channels from native tissue have selective permeabilities, partially based on pore diameter, that discriminate among cytoplasmic second messenger molecules. Permeability was assessed by measurement of selective loss/retention of tracers from liposomes containing reconstituted connexin channels. The tracers employed were tritiated cyclic nucleotides and a series of oligomaltosaccharides derivatized with a small uncharged fluorescent moiety. The data define different size cut-off limits for permeability through homomeric connexin-32 channels and through heteromeric connexin-32/connexin-26 channels. Connexin-26 contributes to a narrowed pore. Both cAMP and cGMP were permeable through the homomeric connexin-32 channels. cAMP was permeable through only a fraction of the heteromeric channels. Surprisingly, cGMP was permeable through a substantially greater fraction of the heteromeric channels than was cAMP. The data suggest that isoform stoichiometry and/or arrangement within a connexin channel determines whether cyclic nucleotides can permeate, and which ones. This is the first evidence for connexin-specific selectivity among biological signaling molecules.

The molecular basis of the intercellular signaling mediated by gap junction channels is a key question in cell biology (*cf.* Ref. 1). Gap junction channels are formed by connexin protein, of which there are at least 15 isoforms (2, 3). Each junctional channel is composed of two anti-symmetric end-to-end hemichannels (connexons), which are hexamers of connexin (4–6). Recordings of single junctional channels show that each isoform generates channels with a characteristic “fingerprint” of conductances (7). A junctional channel typically has a maximal conductance and one or more subconductance states (*cf.* Ref. 8), the occupancy of which may be influenced by voltage (*cf.* Refs. 9 and 10) and/or phosphorylation (*cf.* Refs. 11–14). The number of connexin isoforms, their tissue-specific distributions, and their differential temporal expression suggest that the intercellular molecular signaling mediated by each isoform

is unique. This is substantiated by the observation that genetic defects in each isoform produce distinct developmental and/or physiological defects (15, 16).

We report here investigation of molecular permeability of channels formed by connexin-32 and connexin-26. Defects in connexin-32 are responsible for a human demyelinating peripheral neuropathy (17). Suppression of connexin-26 function is associated with non-syndromic sensorineural human deafness (18). Both connexins seem to act as tumor suppressors (19–22).

Distinct isoform-specific channel conductances imply different pore permeation pathways, and therefore different molecular selectivities. Differences in molecular selectivity are likely to be responsible for key differences in molecular signaling. Understanding of intercellular signaling mediated by connexin channels will be greatly facilitated by discovery of the connexin-specific molecular selectivities and their physical bases.

Most comparative studies of connexin channel permeability have documented junctional permeabilities either to ions (*e.g.*, K^+ , Cl^- , NH_4^+) much smaller than most biological signaling molecules, or to large, charged fluorescent tracers (*e.g.* Lucifer Yellow²⁻, DAPI²⁺) (*cf.* Refs. 23–26). For the former, the observed modest selectivities are intriguing but may not reflect the selectivities among biological signaling molecules, which are larger and have more complex structures and chemistries. For the latter, it is difficult to distinguish the roles played by size and charge in selectivity, and the consequent selectivity among cytoplasmic molecules must be inferred. The fact that both ends of junctional pores are in cytoplasm has made it difficult to obtain unambiguous and detailed *in situ* selectivity data.

A set of homologous uncharged fluorescent tracers of graded sizes was used to define the size selectivity (specifically independent of charge) of connexin channels purified from native tissue. The tracers were loaded into unilamellar liposomes, a significant fraction of which contained affinity-purified reconstituted functional connexin channels. By a transport-specific fractionation (TSF) assay (27–29), liposomes were separated into two populations: those with functional large channels and those without functional channels. Selective permeability among the tracers was determined by direct comparison of the tracers retained by the two populations of liposomes. The studies reported here used two connexin preparations, one containing channels of a single connexin isoform (Cx32¹; from rat

* This work was supported in part by National Institutes of Health Grant GM36044 and Office of Naval Research Grant N00014-90-J-1960 (to A. L. H.). The costs of publication of this article were defrayed in part by the payment of page charges. This article must therefore be hereby marked “advertisement” in accordance with 18 U.S.C. Section 1734 solely to indicate this fact.

¶ Present address: Bundesministerium für Bildung, Wissenschaft, Forschung und Technologie, 53175 Bonn, Germany.

** To whom correspondence should be addressed.

¹ The abbreviations used are: Cx, connexin; $\alpha(1\rightarrow4)Glc_n$, $\alpha(1\rightarrow4)$ -linked glucose linear oligomer, where n is the number of glucose units; DSP, dithiobis(succinimidyl propionate); DTSSP, dithiobis(sulfosuccinimidyl propionate); DTT, dithiothreitol; HPLC, high performance liquid chromatography; mouseCx, connexin immunopurified from mouse liver (Cx32/Cx26); PA, aminopyridyl moiety; PA-sugar, oligomaltose labeled

liver), and one containing channels of mixed isoforms (Cx32/Cx26; from mouse liver). The results establish a connexin-specific difference in pore diameter and provide compelling evidence for heteromeric channels (channels composed of more than one isoform). These differences in selectivity were further explored using tritiated cyclic nucleotide tracers. The data show that connexin channel permeability to cyclic nucleotides, and selectivity among them, is influenced by isoform composition.

EXPERIMENTAL PROCEDURES

Materials—*L*- α -Phosphatidylcholine from soybean (azolectin), egg phosphatidylcholine, bovine brain phosphatidylserine, and lissamine rhodamine B-labeled egg PE were purchased from Avanti Polar Lipids, Inc. Tween 20, nitro blue tetrazolium, and diisopropyl fluorophosphate were obtained from Sigma. Octylglucoside was from Calbiochem Corp. Bio-Gel (A-0.5m, 100–200-mesh, exclusion limit 500,000 Da) was purchased from Bio-Rad. Alkaline phosphatase-conjugated goat anti-mouse IgG and 5-bromo-4-chloro-3-indolyl phosphate were purchased from Boehringer Mannheim. CNBr-activated Sepharose beads were obtained from Pharmacia Biotech Inc. and Immobilon-P transfer membrane from Millipore. Rats and mice were obtained from Taconic Labs. [8,5-³H]cGMP and [2,8-³H]cAMP were obtained from NEN Life Science Products.

Immunopurification of Connexin—Connexin-32-containing structures were immunopurified from rodent livers by a published procedure (29). In brief, a crude membrane fraction was prepared from livers of ~375–100-g female Sprague-Dawley rats or ~16 10–12-week-old Swiss Webster fBR outbred mice. The crude membrane fraction was solubilized in 80 mM octylglucoside and the supernatant, following centrifugation at 100,000 $\times g$ for 45 min, was applied to a column containing Sepharose beads with an attached murine monoclonal antibody directed against Cx32 (M12.13), which does not cross-react with any other connexin (30). Following extensive rinsing, bound connexin was eluted from the antibody by brief exposure to pH 4 buffer. The eluent was rapidly neutralized by dropping directly into 1 M HEPES (pH 7.5). Final HEPES concentration was ~100 mM.

Gel Electrophoresis, Protein Blots, and Immunoblots—These techniques were carried out as described in detail by Rhee *et al.* (29). Proteins were separated by discontinuous polyacrylamide gel electrophoresis (4% (w/v) stacking gel, 13% (w/v) separating gel) and electrotransferred to Immobilon polyvinylidene difluoride membrane. For staining of total protein, blots were blocked with 0.3% Tween 20 in PBS and stained with colloidal gold (0.01% (w/v)). For immunostaining, blots were blocked with PBS-Tween 20 (0.5% (v/v)) and then incubated with primary antibody. After washing with PBS-Tween 20 (0.05% (v/v)) blots were incubated with secondary antibody (alkaline phosphatase-conjugated goat anti-mouse IgG), washed, and developed in 0.1 mg/ml nitro blue tetrazolium and 0.05 mg/ml 5-bromo-4-chloro-3-indolyl phosphate.

Antibodies—The monoclonal antibody used in the immunoaffinity purification and for specific staining of connexin-32 on Western blots (M12.13) is directed against a cytoplasmic domain of Cx32 (30). The antibody used to specifically detect Cx26 on Western blots was a sequence-specific polyclonal directed against the cytoplasmic loop of Cx26 (residues 108–122) (31). The antibody used to detect both connexins on Western blots was a sequence-specific polyclonal antibody directed against an extracellular domain (residues 116–185) conserved in Cx32 and Cx26 (32).

Purification of Plasma Membrane for Cross-linking Studies—Plasma membranes were isolated from rat and mouse livers according to Goodenough (33) and Fallon and Goodenough (34). In brief, liver homogenate was pelleted at 11,000 $\times g$ and then rinsed and centrifuged at 6,000 $\times g$ to remove mitochondria and other small organelles. The final pellet was applied to a sucrose step gradient (55%, 50%, 45%, and 37% sucrose). Plasma membranes were collected at the 37%/45% interface and rinsed twice.

Cross-linking Studies—For cross-linking of purified connexin, two lysine-specific cleavable cross-linking agents were used in combination: DSP, which is lipophilic, and DTSSP, which is water-soluble (Pierce). The cross-linkers were added to the connexin samples (which were ~10 mg/ml in 80 mM octylglucoside and 1 mg/ml phospholipid) from stock

solutions (DSP in Me₂SO, DTSSP in 0.1 M HEPES, pH 7.7) to final concentrations of 0.5–2 mM. Following incubation for 30 min at room temperature, the reaction was stopped by addition of one-sixth reaction volume of 0.5 M lysine in 0.1 M Tris, pH 8.2. Following 10 min of incubation, two-thirds volume of SDS-polyacrylamide gel electrophoresis sample buffer (without DTT) was added. To cleave the cross-linkers, sample buffer containing 100 mM DTT was used and the sample boiled prior to being loaded on the gel. The cross-linkers span a maximal distance of 12 Å.

Connexin in plasma membranes were cross-linked by addition of 0.1 ml of DSP (20 mM in Me₂SO) and 0.1 ml of DTSSP (20 mM in 0.1 M HEPES, pH 7.7) to 2 ml of plasma membrane suspension at a protein concentration of 10 mg/ml, giving a final cross-linker concentration of 2 mM. Cross-linking proceeded for 45 min at room temperature, and was stopped as above. The membranes were then solubilized by addition of 1 volume of 160 mM octylglucoside in 50 mM sodium phosphate, 50 mM NaCl, 5 mM EDTA, 1 mM β -mercaptoethanol, pH 7.2, and incubated at 4 °C for 30 min. The solution was spun at 100,000 $\times g$ for 45 min. The supernatant was applied to the immunoaffinity column and purified for connexin-32-containing structures.

For the cross-linked material, SDS-polyacrylamide gel electrophoresis was performed either on 13% polyacrylamide gels at 200 V for 72 min or on 4–15% gradient gels (Julie) at 200 V for 55 min. Semidry transfer to Immobilon membrane was at 130 mA per minigel for 36 min (13% gels) or for 50 min (4–15% gradient gels). The blots were stained either for total protein with colloidal gold or with antibodies against Cx32 and/or Cx26.

Reconstitution of Purified Connexin into Unilamellar Phospholipid Liposomes—Liposome formation and protein incorporation followed the protocol of Mimms *et al.* (35), as modified by Harris *et al.* (28) and Rhee *et al.* (29). Liposomes were formed by gel filtration of a 1 mg/ml mixture of phosphatidylcholine, phosphatidylserine, and rhodamine-labeled phosphatidylethanolamine at a molar ratio of 2:1:0.03 in urea buffer (see below) containing 80 mM octylglucoside and immunoaffinity-purified connexin. The protein-lipid-detergent mixture was applied to a Bio-Gel A-0.5m column pretreated with sonicated liposomes. The connexin-containing liposomes were collected in the void volume. The size distribution of liposomes was established by filtration over a calibrated TSK G6000PW HPLC column (36) to be highly monodisperse with an approximate mean diameter of 900 Å. The protein/lipid ratio of the liposomes was approximately 1:60 (w/w), corresponding to an amount of connexin equivalent to ~1 hemichannel/liposome. We intentionally worked at a protein/lipid ratio that produced some liposomes that contained functional channels and some that did not (for use as internal controls for tracer trapping and nonspecific leak).

Loading of Liposomes with Tracers—Tracers were loaded into the liposomes by incubation with 5% (v/v) Me₂SO, followed by removal of Me₂SO and untrapped tracers by gel filtration. Control experiments showed that this treatment did not affect connexin channel activity or the behavior of liposomes in the TSF assay. A mixture of the oligosaccharide tracers was loaded into the liposomes at a nominal concentration of 10 mg/ml. Radiolabeled nucleotide tracers were dried from 50% ethanol (v/v) stocks under argon before loading into liposomes at a nominal concentration of 16 μ M.

Transport-specific Fractionation (TSF)—The procedure used to fractionate liposomes into two populations based on sucrose-permeability is described and fully characterized by Harris *et al.* (27, 28) and Rhee *et al.* (29). The principle of using a density shift to fractionate liposomes was adapted from Goldin and Rhoden (37). Linear iso-osmolar density gradients were formed from urea and sucrose buffers in 4.4-ml ultracentrifuge tubes using a Hoefer gradient maker. Urea buffer contained 10 mM KCl, 10 mM HEPES, 0.1 mM EDTA, 0.1 mM EGTA, 3 mM sodium azide, and 459 mM urea at pH 7.6. Sucrose buffer was identical to the urea buffer, except that an osmotically equivalent concentration of sucrose (400 mM) was substituted for the urea. Osmolality of urea and sucrose buffers was 500 mOsm/kg, and their specific gravities (D_4^{20}) were measured to be 1.0056 and 1.0511, respectively, by refractive index and gravimetric methods.

An aliquot of the liposomes (typically 200 μ l) was layered on each gradient. Gradients were typically centrifuged at 300,000 $\times g$ for 3–5 h in a swinging bucket rotor (Sorvall TST 60.4, DuPont) at 4 °C. Liposome bands were recovered by aspiration. The distribution of the liposomes in the gradient was calculated from the specific intensity of rhodamine fluorescence (Perkin-Elmer 650–10S spectrofluorometer; 560 nm excitation and 590 nm emission) and the volume of each collected band.

During the centrifugation, liposomes not permeable to sucrose move into the gradient a short distance, being buoyed by the (lighter) entrapped urea buffer and form a band in the upper part of the gradient.

with an aminopyridyl group; *n*-PA, PA-sugar where *n* is the number of saccharide units; PBS, phosphate-buffered saline; ratCx, connexin immunopurified from rat liver (Cx32); TSF, transport-specific fractionation of liposomes.

Permeable liposomes continuously equilibrate their internal solution with the external solution, and move to a position in the lower part of the gradient corresponding to the density of the liposome phospholipid membrane. Equilibration of extraliposomal and intraliposomal osmolytes through pores the dimensions of hemichannels is very rapid (<1 ms for these liposomes). Therefore, even a channel that opens infrequently will mediate full exchange of osmolytes and cause liposome movement to the characteristic lower position. The protein/lipid ratios used yielded functional channels in 30–50% of the liposomes.

Oligosaccharide Tracers—A maltooligosaccharide mixture consisting chiefly of maltose ($\alpha(1\rightarrow4)\text{Glc}_2$) through maltopentaose ($\alpha(1\rightarrow4)\text{Glc}_5$) was fluorescently labeled by pyridylation according to Hase *et al.* (38). The fluorescent adducts are labeled at the reducing ends of the oligosaccharides and result in linearization of the reducing-end glucose. Stocks were frozen for later use after HPLC chromatograms were run to verify purity.

Recovery of PA-labeled Sugars from Liposomes—Aliquots from bands of vesicles recovered from spun density gradients were diluted 1:1 with HPLC-grade methanol and vortexed to lyse vesicles and disperse lipid as micelles. The mixture was slowly passed through a tC18 Sep-Pak Vac solid phase extraction cartridge (Waters Corp.) pre-equilibrated in methanol, followed by 50% methanol in water to remove lipid. The eluent containing the sugars was next incubated for 30 min with vortexing at room temperature with 50 mg of H-form AG 50W-X2 biotechnology grade cation exchange resin (Bio-Rad) to bind the PA-sugars (positively charged at low pH of resin) as well as other cations. The resin was transferred to a small fritted column and washed with water. Material was eluted from the resin by treatment with 2.5 M ammonium hydroxide for 1 min with agitation, followed by a second wash in ammonia and vacuum recovery of the sample. The samples were speed-vacuumed to dryness and brought up in water for fluorescence quantitation.

Measurement of Tracers—The PA-sugars were quantitatively analyzed on a normal-phase amide-80 HPLC column by monitoring PA fluorescence. 2-PA, 3-PA, 4-PA, and 5-PA (abbreviation: *n*-PA, where *n* is the number of saccharide units) were eluted at 6.8, 8.3, 10.6, and 13.5 min, respectively, with a 70% to 60% gradient of acetonitrile in 3% aqueous triethylammonium acetate, pH 7.3 (modified from Ref. 38). Quantitation was performed by calculation of areas under Gaussians simultaneously fit to eluted peaks. The mole fractions of the entrapped PA tracers were as follows: 2-PA, 0.18; 3-PA, 0.35; 4-PA, 0.16; 5-PA, 0.31.

To determine loss of radiolabeled tracers, the [^3H activity]/[rhodamine fluorescence] ratios were measured for the upper and lower TSF bands in each experiment, and normalized to give the fractional retention of tracers in the lower band relative to that of the upper band. Liposome bands were recovered in approximately 0.75 ml, added to 5 ml of liquid scintillation mixture (Ultima Gold, Packard), thoroughly mixed by vortexing, and the ^3H activity measured in either a Packard TriCarb model 2250CA or model 2700TR liquid scintillation counter (counting window, 0–18.6 keV). Blank controls of 0.75 ml of aqueous buffer and 5 ml of mixture were counted between samples. Counting times were 30 min. The minimum detectable activity, the net signal that can be detected at the 95% confidence level, is approximately given by $\sqrt{8N/t}$ (39), where *N* is the background noise (counts/min) and *t* is the maximum counting time (min). For the present data, *N* = 12.4 and *t* = 30, resulting in a minimum detectable activity of 1.8 cpm. Counting rates were corrected for quench (external standards method) and background. Quench correction was made by measuring the relative activities of a series of uniform, traceable standards (Tritium Reference Source NES-004, [^3H]toluene) quenched to various degrees with nitromethane. The calculated ^3H counting efficiencies were plotted against the transformed spectral index of the external ^{137}Cs standard for each quenched sample in the series, and the data were fitted by a second degree polynomial using a non-linear least squares fit. Quenching corrections of the data sets were made from the transformed spectral index of the external ^{137}Cs standard reported for each sample. Additionally, verification of direct measurements reported as disintegrations per minute using the TriCarb 2250CA (low background model, using preprogrammed Ultima Gold quench data from standards prepared by Packard) was made by comparison of data with the manual quench correction method outlined above.

RESULTS

Co-purification of Connexin-32 and Connexin-26—Connexin was immunoaffinity-purified from octylglucoside-solubilized plasma membrane of rat or mouse liver using a Cx32-specific

monoclonal antibody (29). Gel filtration studies showed that the purified connexin was predominantly in structures the size of single hemichannels (hexamers of connexin) (29). The liposomes were unilamellar (35), and, for a given protein/lipid ratio, the number of permeable liposomes was too great for the functional channels to be formed by dodecamers (29). We infer that the permeabilities described below are those of hemichannel-sized connexin structures (there is strong evidence that connexin hemichannels function in the plasma membrane of cells that express connexin endogenously (40–42) or heterologously (*cf.* Refs. 43–48)). Rat liver gap junctions contain predominantly Cx32 and a small amount of Cx26. Mouse liver junctions contain a much higher ratio of Cx26 to Cx32 (49, 50). Both connexins can be found in the same junctional plaques (32, 50–54).

Applied to rat liver, this procedure yielded Cx32 without detectable non-connexin protein (Fig. 1A). In some purifications, a small amount of Cx26 was recovered. In this study, only rat liver connexin preparations (ratCx) that contained no detectable Cx26 were used.

Applied to mouse liver, this procedure yielded significant amounts of both Cx32 and Cx26 (Fig. 1A). The mouse-derived connexin (mouseCx) is a co-expressed mixture of Cx26 and Cx32. Since the immunopurification used a monoclonal antibody specific for Cx32 that does not cross-react with Cx26 (Ref. 30; demonstrated in Fig. 1A), the copurification of Cx26 along with Cx32 suggested that the two isoforms were in the same heteromeric structures.

The relationship between the two connexin isoforms in purified mouseCx was explored using cleavable bifunctional cross-linking reagents. The two isoforms could be reversibly cross-linked together in dilute solution (Fig. 1B) (55). Under these conditions, cross-linking within oligomers is very much favored over cross-linking between oligomers (56). This result supports the idea that the purified mouseCx structures have a substantial heteromeric component, and raises the possibility that heteromeric channels exist *in situ*.

This was addressed by studies in which plasma membranes were exposed to mild cross-linking conditions prior to detergent solubilization (55). This protocol cross-links hemichannel connexin monomers while in plasma membrane, preserving their *in situ* structural relationships; subsequent subunit exchange is unlikely to occur. This controls for possible subunit exchange between solubilized hemichannels, as has been noted for a few oligomeric membrane proteins in the presence of detergent (57–59). After solubilization, the cross-linked material was immunoaffinity-purified for Cx32-containing structures, as before. After purification, cleavage of cross-linkers revealed Cx26 (Fig. 1C). If the two isoforms had been present in the tissue in entirely distinct populations of homomeric hemichannels, Cx26 would not have been recovered. To minimize the potential for cross-linking between apposed or neighboring hemichannels, the studies were carried out under conditions of considerably less than maximal cross-linking; after cross-linking, a significant amount of connexin remained in structures smaller than hemichannels (Fig. 1C, lane 1).

Because of the co-purification of non-cross-linked connexin, and because the same qualitative results were obtained with and without prior cross-linking in the plasma membrane, we consider it likely that heteromeric structures are found *in situ*. The combination of more than one connexin isoform in the same hemichannel structure may provide a structural basis for cellular modulation of junctional channel physiology by variation of the relative amounts of each connexin isoform in junctional channels.

Transport-specific Fractionation (TSF)—The molecular se-

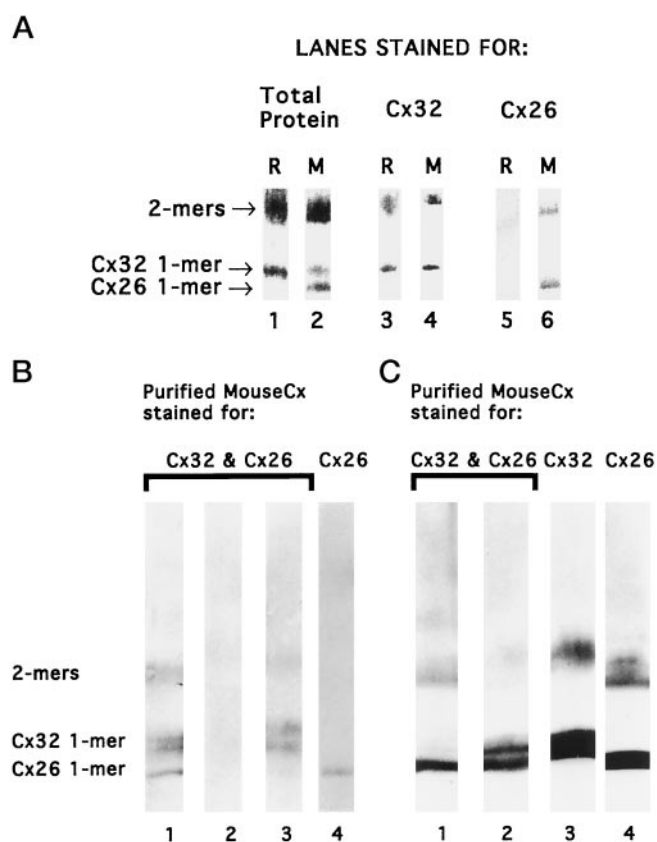


FIG. 1. *A*, Western blots of immunopurified connexin from rat (*R*) and mouse (*M*) liver. Lanes 1 and 2 are stained for total protein with colloidal gold. Lanes 3 and 4 and lanes 5 and 6 are immunostained for Cx32 and Cx26, respectively. The immunoaffinity purification yields Cx32 from rat liver and a mixture of Cx32 and Cx26 from mouse liver. Connexin was purified from octylglucoside-solubilized plasma membrane using a Cx32-specific monoclonal antibody. *B*, cross-linking of Cx26 and Cx32 in immunoaffinity-purified mouseCx. Blots are of connexins separated on 4–15% polyacrylamide gradient gels. Lane 1, purified mouseCx prior to cross-linking. Lane 2, same material as lane 1 after cross-linking with cleavable bifunctional cross-linkers DTSSP and DSP (0.1 mM each). Protein concentration was 10 μ g/ml. Lane 3, same material as lane 2 after splitting of cross-linkers with 100 mM DTT. Lanes 1–3 are stained with an antibody against an epitope shared by Cx32 and Cx26. In Cx26, the epitope is apparently masked by the cross-linkers, so the same material as in lane 3 is shown in lane 4 stained with the Cx26-specific antibody specific to identify its position. With cross-linking, monomeric and dimeric connexin bands virtually disappear (lane 2); silver stains of the gels showed that the cross-linked protein did not significantly enter the gel. Monomeric Cx26 and Cx32 reappear with splitting of the cross-linker (lanes 3 and 4). *C*, exposure of mouse plasma membrane to cross-linkers prior to immunopurification suggests that Cx32 and Cx26 are in the same structures *in situ*. Blots are of connexins separated on 4–15% acrylamide gradient gels. Lane 1, mouseCx immunopurified from mouse liver plasma membranes after exposure to the same cross-linkers as in *B*. Protein concentration was 10 mg/ml and cross-linkers were 1 mM each. Lane 2, same material as lane 1 following splitting of the cross-linkers with 100 mM DTT. Lanes 1 and 2 are stained with the same antibody that recognizes both Cx32 and Cx26 as used in *B*. Lanes 3 and 4, same material as lane 2 stained with the antibodies specific for Cx32 and Cx26, respectively. Under these conditions, the Cx32 was cross-linked to a much greater degree than was the Cx26; monomeric Cx32 is absent in lane 1. The higher molecular weight forms of both connexins are due to the cross-linking (lane 1), shown by the shift to lower molecular weight forms upon splitting of the cross-linkers (lane 2).

lectivities of channels formed by ratCx and mouseCx were explored and compared by a tracer-flux technique used in combination with transport-specific liposome fractionation. Purified connexin was incorporated into unilamellar liposomes by gel filtration of octylglucoside-solubilized lipid and connexin (28, 35). Liposomes containing functional channels were sepa-

rated from liposomes without functional channels by TSF achieved by centrifugation through an iso-osmotic density gradient formed by urea and sucrose solutions (see “Experimental Procedures”) (27, 28). In this assay, liposomes that do not contain functional channels (*i.e.* are not permeable to the density-conferring osmolytes of the gradient, urea and sucrose) migrate to an equilibrium position in the upper part of the gradient, determined by their density. This density is a volume-weighted sum of the densities of the entrapped urea buffer and the more dense phospholipid membrane. For liposomes that contain large open pores, the osmolytes exchange across the liposome membrane through the open channels. These liposomes migrate to a lower equilibrium position, determined by lipid density.

Limiting Pore Diameters—The limiting dimensions of the channel pores were examined using a series of oligomaltosaccharides (two to five glucose units) derivatized with an aminopyridyl group (PA), a small, highly fluorescent moiety uncharged at physiological pH. X-ray studies, solution NMR studies, and computer modeling show that, with increasing oligomeric number, these compounds form rigid helical structures with a full turn requiring at least six saccharide units (60–62). Thus, the axial cross-sectional areas of this series of tracers increase with oligomeric number (Fig. 2).

Liposomes were loaded with the tracers and fractionated by the TSF into two populations, one containing liposomes without functional channels, and one containing liposomes with functional channels. The amounts of tracers in the two populations of liposomes were determined by fluorescence quantitation of HPLC-separated tracers. A tracer was considered permeable if it was lost from the liposomes in the lower band (the population with functional channels) and retained by those in the upper band (the population without functional channels) (*center graphic* in Fig. 3). The tracers in the upper band of liposomes served as internal controls for the amounts of tracers trapped. Because of this, determination of permeability in this system is insensitive to large variations in the number of active channels (*e.g.* proportion of liposomes in each band). It is also insensitive to large variation in channel open time because solute equilibration between the intraliposomal and extraliposomal solutions through an open channel is very rapid (<1 ms for these liposomes).

Liposomes without functional ratCx or mouseCx channels retained all four PA-sugars in the same ratios (Fig. 3, *upper panels*), which matched those in the loading solution (data not shown). However, liposomes containing functional channels from mouseCx or ratCx showed differential retention of PA-sugars (Fig. 3, *lower panels*). The mouseCx liposomes lost the smallest tracer, and retained the three largest ones in the “loaded” stoichiometric ratios. The ratCx liposomes lost the two smallest tracers and retained the two largest tracers, in stoichiometric ratio.

The upper size limit for Cx32 (ratCx) channels is thus bracketed by the sizes of the 3-PA and 4-PA sugars, and the upper size limit for channels that also contain Cx26 (mouseCx) is bracketed by 2-PA and 3-PA. The data show that channels formed solely by Cx32 have a larger limiting pore diameter to uncharged permeants than do channels that also contain Cx26. We conclude that Cx26 contributes to a pore of narrowed limiting cross-sectional dimension.

The PA-sugar data also show that all the purified mouseCx channels were heteromeric; there was no detectable loss of 3-PA by the mouseCx liposomes containing functional channels. Since homomeric Cx32 channels were shown by the ratCx data to be permeable to 3-PA, any such channels in the mouseCx liposome population would have reduced the amount

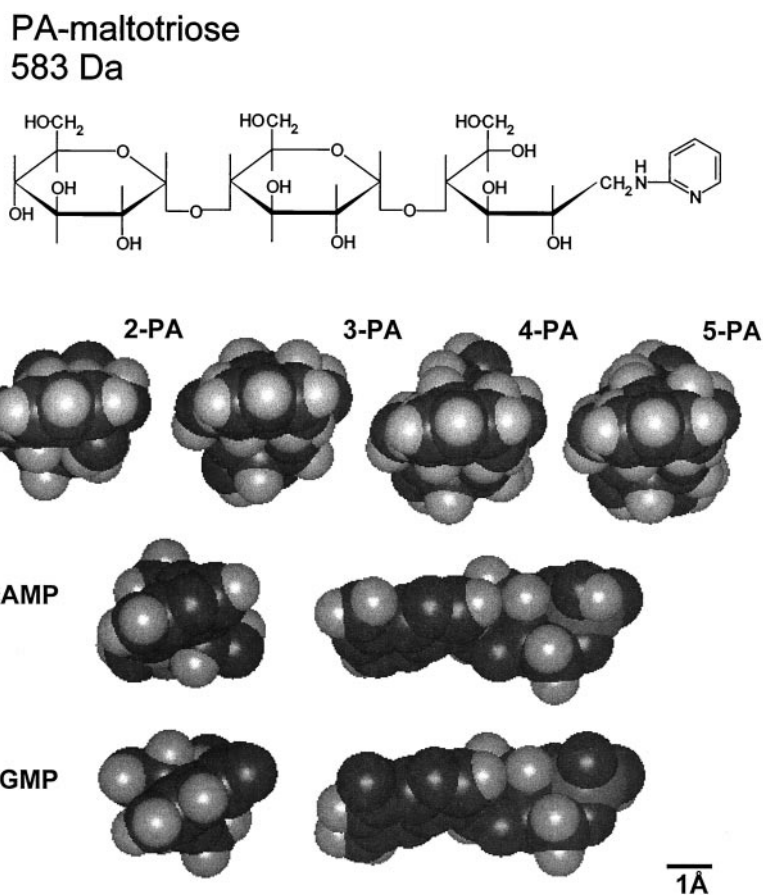


FIG. 2. Structures of the tracers. Row 1, Hayworth projection of PA-maltotriose (3-PA), one of the oligosaccharide tracers. Row 2, molecular models of the PA-sugar tracers shown in minimal axial cross-section from the PA-derivatized (reducing) end. Left to right, di-, tri-, tetra-, and penta-saccharides. Structures were composed using the Biopolymer module of InsightII according to the average torsion angles derived from solution NMR, x-ray, and computational studies (60–62). The aminopyridyl group is conjugated by reductive amination at the reducing-end sugar, which becomes uncyclized. Rows 3 and 4, molecular models of cAMP and cGMP, showing minimal axial cross-sectional and longitudinal views.

of 3-PA retained relative to the two larger tracers. This was not the case, which indicates that, to the limit of measurement resolution ($\sim 2\%$), there were no homomeric Cx32 channels in the mouseCx population; all were heteromeric Cx32/Cx26 (homomeric Cx26 is unlikely, since the purification is specifically for Cx32-containing structures). The result could also be explained by mouse Cx32 having different permeability properties than rat Cx32, but since they have identical amino acid sequences (63), this is unlikely.

Because the PA tracers are uncharged and their chemistries identical, the selectivities described thus far must arise from size considerations alone. Using the average torsion angles derived from NMR, x-ray, and computational studies (60–62), the calculated minimum axial cross-sections (in projection) from van der Waals models of 2-PA, 3-PA, and 4-PA are $4.4 \text{ \AA} \times 3.4 \text{ \AA}$, $4.4 \text{ \AA} \times 3.8 \text{ \AA}$, and $4.4 \text{ \AA} \times 4.0 \text{ \AA}$, respectively. Selectivity in this size range may be important for biological signaling. Charged permeants close to the limiting dimensions of the pore may interact significantly with the pore walls. For such permeants, the roles of formal charge and chemical affinity could impart a higher degree of specificity of selectivity than would be expected from size considerations alone. The minimum projected axial cross-sectional dimensions of cAMP, inositol 1,4,5-trisphosphate, and ATP bracket those of the tracers used in this study ($3.6 \text{ \AA} \times 3.2 \text{ \AA}$, $4.4 \text{ \AA} \times 3.4 \text{ \AA}$, and $5.6 \text{ \AA} \times 4.5 \text{ \AA}$, respectively).

Permeability to Cyclic Nucleotides—Using radiolabeled tracers, permeabilities to two cyclic monophosphate nucleotides were compared. Tritiated cAMP or cGMP was loaded into the liposomes, and their permeabilities through the reconstituted channels determined as for the PA sugars. As before, tracer retained by liposomes without functional channels served as an internal control. For homomeric Cx32 liposomes, no cAMP or cGMP label above background levels was retained by liposomes

with functional channels (Fig. 4A). This demonstrates permeability of cAMP and cGMP through Cx32 channels. However, for the heteromeric Cx32/26 channels, the liposome population with functional channels lost 26% of the entrapped cAMP, and 72% of the entrapped cGMP (Fig. 4B).

The time for tracer efflux from liposomes containing channels is many orders of magnitude less than the time required to complete the TSF. Therefore, this is a steady-state measurement of permeability. The difference in partial losses of the nucleotide tracers indicates that different fractions of the heteromeric channel population were permeable to each; 26% of the liposomes were permeable to cAMP, and 72% were permeable to cGMP.

The data indicate heterogeneous selectivities among second messengers within the heteromeric channel population. A reasonable explanation is that the heteromeric channel population is composed of a variety of isoform stoichiometries and/or arrangements. The data suggest that some of these variations in channel structure determine permeability to cyclic nucleotides. Since different fractions of the liposomes were permeable to cAMP or cGMP, the data also suggest that the structural differences in the channels permit discrimination between cAMP and cGMP. This is the first evidence that connexin channels can have different permeabilities for different biological second messenger molecules, and suggests that the selectivity is determined by stoichiometry and/or arrangement of isoforms composing the channel.

Since homomeric Cx32 channels are permeable to both cyclic nucleotides and some of the heteromeric channels are not, one expects that, if the fraction of Cx26 composing each heteromeric channel were increased, more channels would be impermeable to the cyclic nucleotides. Control of the channel Cx26:Cx32 stoichiometry would be possible if one were able to form channels from specified ratios of connexin monomers. In the

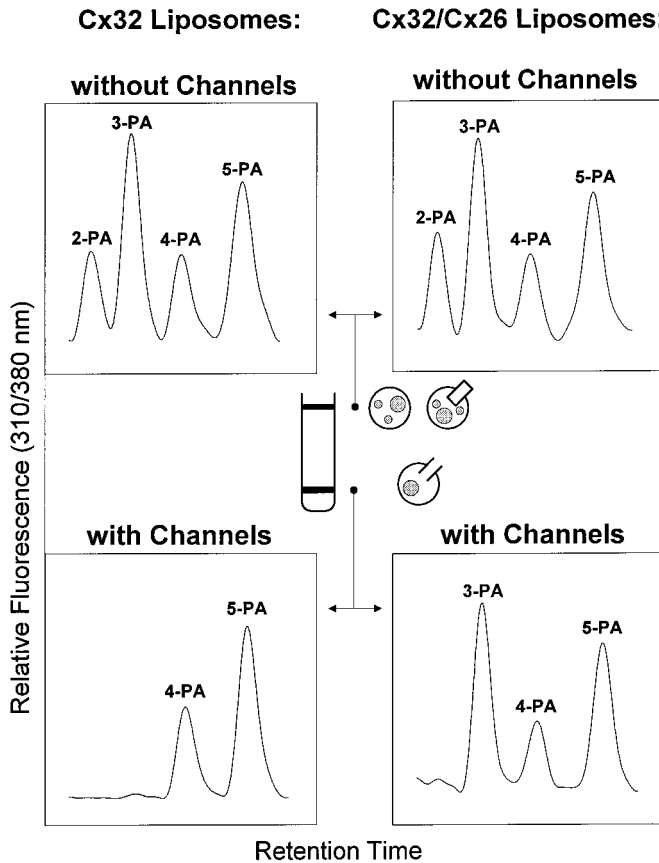


FIG. 3. HPLC chromatograms of PA-sugars retained by liposomes showing differential permeability. Upper panels are for liposomes not containing functional channels (upper band of TSF). Lower panels are for liposomes containing functional channels (lower band). Data from liposomes containing ratCx are on the left, and mouseCx on the right. The upper traces are internal controls for the complement of tracers trapped. The graphic in the center shows how permeability to entrapped trappers is assessed using a TSF gradient. Liposomes with entrapped tracers are centrifuged through an iso-osmolar density gradient formed from a urea solution (non-chaotropic concentration) and an osmotically equivalent sucrose solution. Liposomes without functional channels form a band in the upper part of the gradient. Liposomes that have functional channels equilibrate the intraliposomal solution with the external solution, and form a band at a lower position determined solely by lipid density. These liposomes will have lost any tracers permeable through their channels, whereas the liposomes in the upper band will retain all tracers and thus are internal controls for tracer trapping in each experiment. Comparison of tracers in the lower and upper bands permits assessment of tracer permeability through functional channels (see "Experimental Procedures").

present study, however, channels are purified from native tissue as intact hexamers, not monomers. Channels purified from cells co-expressing different ratios of Cx32 and Cx26 would be useful in this context.

We took advantage of naturally occurring variations in Cx26:Cx32 ratio in a native co-expression system to address this issue. We noted that in the purified connexin from different mouse preparations the ratio of Cx26 to Cx32 was somewhat variable. By carrying out cyclic nucleotide flux studies on different preparations, we hoped to see a direct correlation between Cx26:Cx32 ratio and impermeability to cyclic nucleotides. The form of the relation cannot be predicted because (a) the actual distribution of isoform stoichiometries for a given Cx26:Cx32 ratio is not known, (b) the actual distribution of monomer arrangements within a channel for a given stoichiometry is not known, and (c) the relation between stoichiometry/arrangement and permeability is not known. Nevertheless, a correlation may be evident.

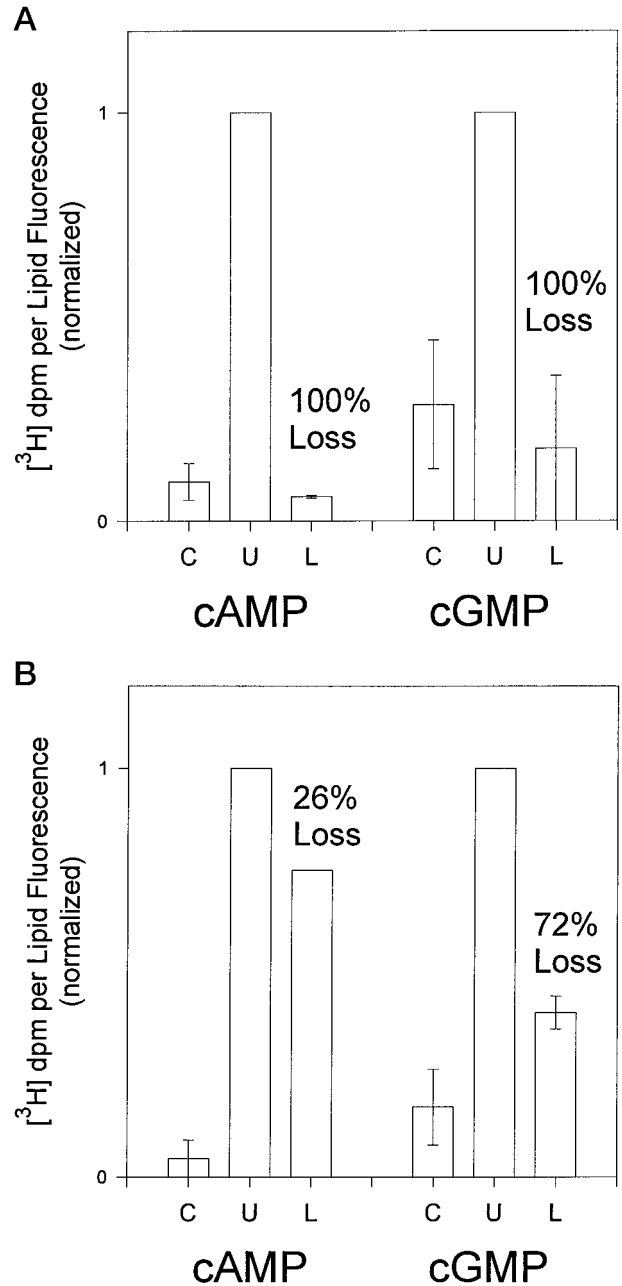


FIG. 4. Cyclic nucleotide tracer flux studies. Connexin-containing liposomes loaded with [^3H]cAMP or [^3H]cGMP were functionally separated by TSF centrifugation. The ratio of ^3H activity to liposome fluorescence (rhodamine-PE) was determined for each sample. The control ratio (C) is the normalized amount of tracer nonspecifically bound to liposomes (values derived from liposomes exposed to tracers without Me_2SO). For the upper band (U; liposomes not containing functional channels), the [^3H activity]/[lipid fluorescence] ratio in excess of that in the control population reflects the net amount of tracer entrapped in liposomes prior to TSF and thus serves as an internal control. This ratio is effectively the tracer loaded per liposome and was normalized to unity (*i.e.* full retention of tracer). For the lower band (L; liposomes containing functional channels) the [^3H activity]/[lipid fluorescence] ratio was normalized to that of the upper band, and represents the fractional retention of tracer in this population of liposomes. For control (C), error bars are standard errors of the measurements. For lower band (L), error bars are standard errors of the normalized measurements. A, data from ratCx liposomes. There was 100% loss of entrapped cAMP and cGMP radiolabel by functional Cx32 channels. B, data from Cx32/Cx26 liposomes. In contrast, most, but not all, of the cAMP radiolabel was retained by the liposomes with functional channels; there was 26% loss. Because this is a steady state measurement, the flux per liposome is all-or-none. Thus, 26% of the Cx32/Cx26 liposomes were permeable to cAMP, and 72% of the same liposome population were permeable to cGMP.

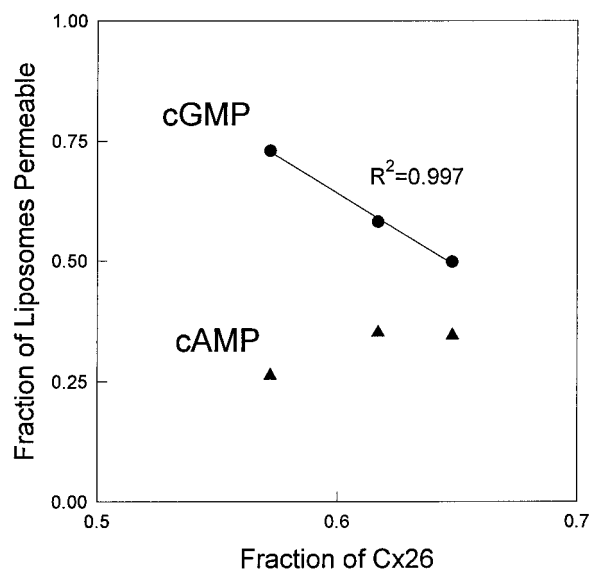


FIG. 5. Relation between permeability to cyclic nucleotides and fraction of Cx26 in the heteromeric channel population. Permeabilities to cAMP and cGMP were determined for three preparations of heteromeric Cx32/Cx26 channels from mouse liver with different Cx26:Cx32 ratios. Fraction of Cx26 relative to total connexin in each was determined from Western blots (see "Experimental Procedures"). The data show that decreased permeability to cGMP correlates well with increased Cx26 content. There is no significant trend for cAMP over this range of Cx26:Cx32 ratios. The differential modulation of cGMP permeability by Cx26 is evident.

The results of this experiment using three different preparations of heteromeric channels are shown in Fig. 5. Ratios of the connexins were determined from quantitative analysis of Western blots stained for total protein with colloidal gold and for connexins with Cx32- and Cx26-specific antibodies. There is a tight, linear correlation between fraction of Cx26 in the preparation and impermeability to cGMP. There is no such correlation with cAMP permeability over this modest range of Cx26:Cx32 ratios. The cGMP data validate the role of connexin isoform composition in selective permeability among intercellular second messengers.

DISCUSSION

Different connexin isoforms have been shown to intermingle within a junctional plaque (53, 54, 64). Formation of heteromeric junctional channels seems firmly established from biochemical and physiological studies on native (65, 66) and transfected cells (67–69). Scanning electron microscopic measurements on purified rodent hemichannel plaques failed to reveal hemichannel masses indicative of heteromeric structures (53), but they may have been masked to some extent by statistical variation in the data.

The cross-linking data presented here support the existence of heteromeric hemichannels in native tissue. Lateral interhemichannel linkages within the same plasma membrane are unlikely except under maximal cross-linking conditions (6) because, even in condensed junctions, the interchannel spacing is wider than the cross-linker length (12 Å) (70–72). Moreover, lateral collisional cross-linking in other membrane protein arrays is rare (73–75). It is possible that interhemichannel linkages could form across the intercellular "gap" if the cross-linker could penetrate this intercellular space. The "gap" is known to be penetrated only by heavy metal stains and sucrose, which are smaller than the cross-linkers (5, 76). Additionally, due to the relative surface areas available for interaction, under mild cross-linking conditions intrahemichannel linkages would be favored over interhemichannel linkages (77).

Junctional channels generally behave as two hemichannels in series from data where properties of hemichannels are directly determined and compared with those of the corresponding junctional channels (45, 46, 48). However, the voltage-dependent gating behavior of heterotypic junctional channels cannot always be predicted from the hemichannel properties inferred from studies of homotypic junctional channels (78). There are no data that address whether hemichannel selectivities are altered when hemichannels form junctional channels. The fluorescent tracers developed for the present study can likely be used in conjunction with maltase inhibitors in cellular studies to directly address this issue.

Inspection of the PA-sugar structures (Fig. 2) shows that with increasing oligomeric number the axial cross-section becomes more circular. Therefore, the impermeability of a tracer may not necessarily be due to a larger cross-sectional major axis, but due to a larger minor axis. Additionally, because of structural differences between the two isoforms, the packing of connexin monomers within heteromeric channels may not be radially symmetric, and may contribute to the selectivities described here. Therefore, the molecular selectivity of homomeric Cx26 channels cannot be inferred; homomeric Cx26 channels may not necessarily have narrower pores than homomeric Cx32 channels. Molecular flexibility, hydration, and other factors in permeation prevent a precise determination of the cross-sectional dimensions of the pores from these studies. However, the differential permeability of the uncharged tracers does serve as an index of relative pore diameter and permits comparison with other potential permeants and other connexin channel pores.

The permeability studies with the PA-sugars do not permit discrimination between a localized size selectivity filter and a decrease in diameter along the entire pore length. The unitary conductance of Cx32 homomeric channels is less than that of homomeric Cx26 channels (79, 80). If the pores were right cylinders, the data would suggest that the Cx26-induced narrowing is localized, and not along the full length of the pore (*i.e.* the structure that produces the size selectivity does not dominate the pore conductance). However, there are data suggesting that connexin pores are not simple right cylinders (23). If selectivity among charged permeants arises from straightforward luminal surface charge considerations (as may be the case for voltage-dependent anion channel; Ref. 81), a narrowed pore would enhance charge selectivity, due to closer approach of charged residues in the pore by permeants.

Cellular and liposome studies are consistent with the data obtained here for uncharged tracers. Data from HeLa cells expressing single murine connexin isoforms probed with several nonhomologous charged tracers (Lucifer Yellow²⁻, DAPI²⁺, neurobiotin^{δ+}, propidium²⁺, ethidium⁺) can be explained by Cx26 having an uncharged pore, and Cx32 having a cationic pore the same size or larger (25). Other studies involving differential permeability through Cx26 and Cx32 channels support the idea of a cationic (*i.e.* anion-selective) Cx32 channel, but do not bear directly on limiting diameter (82, 83). A smaller diameter for Cx26 channels relative to that of Cx32 channels is supported by comparative data using Lucifer Yellow (83). Studies using a different type of permeability assay and different uncharged probes (raffinose, Nycodenz, metrizamide) supports Cx26 contributing to a narrowed pore (84, 85). Elucidation of the structural basis for the difference in limiting dimension must await identification of the pore-lining domains of connexin channels. Recent data suggest that the first transmembrane domain contributes to the pore lumen (86, 87), but inspection of the relevant sequences is not overtly informative as to the basis of the difference in selectivity.

From a biophysical perspective, it will be satisfying to obtain complementary selectivity data for homomeric Cx26 channels. A focus of the present study was to investigate the molecular selectivity (and thereby, the signaling properties) of connexin channels found in native tissue. It is possible that homomeric Cx26 could be purified from murine liver by a Cx26-specific antibody or from transfected cells (88).

Gap junction permeability to cAMP is strongly suspected in several cellular systems (89–91). The connexins involved in those systems have not been positively identified, but the connexins studied here are not among the likely candidates (which are Cx35, Cx37, and Cx43). This is the first study to directly assess permeability to cyclic nucleotides in channels formed by Cx32 or Cx32/Cx26. The cAMP- and cGMP-permeable heteromeric channels may compose separate populations. On the other hand, some cAMP-permeable heteromeric channels may also be permeable to cGMP (*i.e.* the cAMP-permeable channels may be a subset, in whole or in part, of the cGMP-permeable channels). The data do not distinguish between these possibilities.

It would be desirable to have a quantitative model that accounts for the relation between Cx26:Cx32 ratio and cyclic nucleotide permeability. The binomial distribution was used to calculate a possible distribution of channel stoichiometries. The corresponding permeabilities were predicted assuming that (*a*) stoichiometry alone controls permeability, and (*b*) the relation between stoichiometry and change in permeability is linear. The prediction did not obviously match the relations shown in Fig. 5, indicating that the simple assumptions above are invalid. Further analysis of this system will require explicit determination of the distribution of stoichiometries in a channel population. It is surprising that such a small change in the proportion of Cx26 present (8%) generates such a significant change in the number of channels permeable to cGMP (25%).

The narrow range of Cx26:Cx32 ratios in the purified protein may be because each purification of connexin from mouse liver used tissue from 16 animals, possibly averaging over substantial individual variations in connexin-26 content. The use of channels from native tissues, although helpful in establishing the properties of *in situ* channels, places constraints on the range of available isoform ratios. These studies could be extended by the use of heterologous co-expression systems, using fewer animals per preparation (*i.e.* obtaining greater preparation-to-preparation variation in Cx26:Cx32 ratio), or by preparative fractionation of purified channels on the basis of subunit stoichiometry.

The nonselective permeability of cAMP and cGMP through homomeric Cx32 channels is consistent with their wider pore dimensions established by the PA-sugar studies. Similarly, the impermeability of the nucleotides through some of the heteromeric channels does not require any basis other than a narrower pore, also established by the PA-sugar studies. The basis of the selectivity among these nucleotides by heteromeric channels, however, is not likely to be size alone (the size difference between cAMP and cGMP is minimal). The nucleotides have the same net charge, but the charge contours of the purine ring systems differ. Additionally, cAMP can form two hydrogen bonds while cGMP can form three. The selectivity is likely to derive from the different chemistries of the molecules, suggesting the presence of selective binding sites for signaling molecules within connexin pores.

The isoform-dependent molecular selectivity of connexin channels in native tissues demonstrated here, particularly that among second messengers, may be physiologically important. Differential regulation of Cx26 and Cx32 expression occurs in regenerating and differentiating liver, in hepatic tumorigene-

sis, and in cellular growth control (20, 92–97). The data reported here suggest that dynamic regulation of junctional channel composition *in vivo* could effectively and efficiently modulate intercellular signaling mediated by cyclic nucleotides.

Altered or disrupted permeability of cyclic nucleotides through connexin channels is likely to have important consequences. Cx32-deficient mice have increased rates of spontaneous liver tumors and greater sensitivity to carcinogens (22). In humans, genetic defects in Cx32 cause the X-linked form of Charcot-Marie-Tooth disease (a peripheral demyelinating neuropathy) (98). Intriguingly, it has been shown recently that the full disease phenotype can be caused by a point mutation in Cx32 whose only observable effect is to narrow the pore, perhaps sufficiently to exclude cyclic nucleotides, while remaining permeable to salts (87). The distinct roles of each connexin in developmental and pathological processes may arise from differences in molecular signaling mediated, in part, by the selectivities measured and described here.

Acknowledgments—We thank Yuan-Chuan Lee and Jian-Qian Fan for their crucial assistance in the synthesis and HPLC analysis of the PA-sugar tracers, and William H. Biggley for assistance with high accuracy nuclear counting of ³H-labeled tracers. We also thank Daniel Goodenough and David Paul for providing the hybridoma secreting the Cx32-specific monoclonal antibody, and for providing the Cx26-specific affinity-purified antiserum, and Bruce Nicholson for providing affinity-purified antiserum that recognized both Cx32 and Cx26. Use and care of animals was according to institutional guidelines.

REFERENCES

- Kumar, N. M., and Gilula, N. B. (1996) *Cell* **84**, 381–388
- Beyer, E. C., Paul, D. L., and Goodenough, D. A. (1990) *J. Membr. Biol.* **116**, 187–194
- Bruzzone, R., White, T. W., and Paul, D. L. (1996) *Eur. J. Biochem.* **238**, 1–27
- Makowski, L., Caspar, D. L. D., Phillips, W. C., and Goodenough, D. A. (1977) *J. Cell Biol.* **74**, 629–645
- Unwin, P. N. T., and Zampighi, G. A. (1980) *Nature* **283**, 545–549
- Cascio, M., Kumar, N. M., Safarik, R., and Gilula, N. B. (1995) *J. Biol. Chem.* **270**, 18643–18648
- Spray, D. C. (1994) in *Molecular Mechanisms of Epithelial Cell Junctions: From Development to Disease* (Citi, S., ed) pp. 195–215, R. G. Landes, New York
- Veenstra, R. D., and Brink, P. R. (1996) *Biophys. J.* **70**, 1082–1084
- Moreno, A. P., Rook, M. B., Fishman, G. I., and Spray, D. C. (1994) *Biophys. J.* **67**, 113–119
- Bukauskas, F. F., Elfgang, C., Willecke, K., and Weingart, R. (1995) *Biophys. J.* **68**, 2289–2298
- Kwak, B. R., Saez, J. C., Wilders, R., Chanson, M., Fishman, G. I., Hertzberg, E. L., Spray, D. C., and Jongsma, H. J. (1995) *Pflügers Arch.* **430**, 770–778
- Takens-Kwak, B. R., and Jongsma, H. J. (1992) *Pflügers Arch.* **422**, 198–200
- Moreno, A. P., Fishman, G. I., and Spray, D. C. (1992) *Biophys. J.* **62**, 51–53
- Chanson, M., Hermans, M. M. P., and Jongsma, H. J. (1994) *J. Physiol.* **479**, 117P–118P
- Paul, D. L. (1995) *Curr. Opin. Cell Biol.* **7**, 665–672
- Donaldson, P., Eckert, R., Green, C., and Kistler, J. (1997) *Histol. Histopathol.* **12**, 219–231
- Pericak-Vance, M. A., Barker, D. F., Bergoffen, J. A., Chance, P., Cochrane, S., Dahl, N., Exler, M. C., Fain, P. R., Fairweather, N. D., Fischbeck, K., Gal, A., Haites, N., Ionasescu, R., Ionasescu, V. V., Kennerson, M. L., Monaco, A. P., Mostacciuolo, M., Nicholson, G. A., Sillen, A., and Haines, J. L. (1995) *Human Heredity* **45**, 121–128
- Kelsell, D. P., Dunlop, J., Stevens, H. P., Lench, N. J., Liang, J. N., Parry, G., Mueller, R. F., and Leigh, I. M. (1997) *Nature* **387**, 80–83
- Yamasaki, H., Mesnil, M., Omori, Y., Mironov, N., and Krutovskikh, V. (1995) *Mutat. Res.* **333**, 181–188
- Lee, S. W., Tomasetto, C., and Sager, R. (1991) *Proc. Natl. Acad. Sci. U. S. A.* **88**, 2825–2829
- Hirsch, K. K., Xu, C. E., Tsukamoto, T., and Sager, R. (1996) *Cell Growth Diff.* **7**, 861–870
- Temme, A., Buchmann, A., Gabriel, H. D., Nelles, E., Schwarz, M., and Willecke, K. (1997) *Curr. Biol.* **7**, 713–716
- Veenstra, R. D., Wang, H.-Z., Beblo, D. A., Chilton, M. G., Harris, A. L., Beyer, E. C., and Brink, P. R. (1995) *Circ. Res.* **77**, 1156–1165
- Veenstra, R. D., Wang, H. Z., Beyer, E. C., and Brink, P. R. (1994) *Circ. Res.* **75**, 483–490
- Elfgang, C., Eckert, R., Lichtenbergfrate, H., Butterweck, A., Traub, O., Klein, R. A., Hulser, D. F., and Willecke, K. (1995) *J. Cell Biol.* **129**, 805–817
- Veenstra, R. D. (1996) *J. Bioenerg. Biomembr.* **28**, 327–337
- Harris, A. L., Walter, A., and Zimmerberg, J. (1989) *J. Membr. Biol.* **109**, 243–250
- Harris, A. L., Walter, A., Paul, D. L., Goodenough, D. A., and Zimmerberg, J. (1992) *Mol. Brain Res.* **15**, 269–280
- Rhee, S. K., Bevans, C. G., and Harris, A. L. (1996) *Biochemistry* **35**,

- 9212-9223
30. Goodenough, D. A., Paul, D. L., and Jesaitis, L. (1988) *J. Cell Biol.* **107**, 1817-1824
 31. Goliger, J. A., and Paul, D. L. (1994) *Dev. Dyn.* **200**, 1-13
 32. Zhang, J. T., and Nicholson, B. J. (1994) *J. Membr. Biol.* **139**, 15-29
 33. Goodenough, D. A. (1974) *J. Cell Biol.* **61**, 557-563
 34. Fallon, R. F., and Goodenough, D. A. (1981) *J. Cell Biol.* **90**, 521-526
 35. Mimms, L. T., Zampighi, G. A., Nozaki, Y., Tanford, C., and Reynolds, J. A. (1981) *Biochemistry* **20**, 833-840
 36. Ollivon, M., Walter, A., and Blumenthal, R. (1986) *Anal. Biochem.* **152**, 262-274
 37. Goldin, S. M., and Rhoden, V. (1978) *J. Biol. Chem.* **253**, 2575-2583
 38. Hase, S., Ibuki, T., and Ikenaka, T. (1984) *J. Biochem. (Tokyo)* **95**, 197-203
 39. Rivkin, R. B., and Seliger, H. H. (1981) *Limnol. Oceanogr.* **26**, 780-785
 40. Malchow, R. P., Qian, H., and Ripps, H. (1993) *J. Neurosci. Res.* **35**, 237-245
 41. Ebihara, L. (1996) *Biophys. J.* **71**, 742-748
 42. DeVries, S. H., and Schwartz, E. A. (1992) *J. Physiol.* **445**, 201-230
 43. Paul, D. L., Ebihara, L., Takemoto, L. J., Swenson, K. I., and Goodenough, D. A. (1991) *J. Cell Biol.* **115**, 1077-1089
 44. Ebihara, L., and Steiner, E. (1993) *J. Gen. Physiol.* **102**, 59-74
 45. Ebihara, L., Berthoud, V. M., and Beyer, E. C. (1995) *Biophys. J.* **68**, 1796-1803
 46. Gupta, V. K., Berthoud, V. M., Atal, N., Jarillo, J. A., Barrio, L. C., and Beyer, E. C. (1994) *Invest. Ophthalmol. Vis. Sci.* **35**, 3747-3758
 47. Li, H. Y., Liu, T. F., Lazrak, A., Peracchia, C., Goldberg, G. S., Lampe, P. D., and Johnson, R. G. (1996) *J. Cell Biol.* **134**, 1019-1030
 48. Trexler, E. B., Bennett, M. V. L., Bargiello, T. A., and Verselis, V. K. (1996) *Proc. Natl. Acad. Sci. U. S. A.* **93**, 5836-5841
 49. Nicholson, B. J., and Zhang, J.-T. (1988) in *Modern Cell Biology: Gap Junctions* (Hertzberg, E. L., and Johnson, R. G., eds) Vol. 7, pp. 207-218, Alan R. Liss, Inc., New York
 50. Traub, O., Look, J., Dermietzel, R., Brümmer, F., Hulser, D. F., and Willecke, K. (1989) *J. Cell Biol.* **108**, 1039-1051
 51. Nicholson, B. J., Dermietzel, R., Teplow, D., Traub, O., Willecke, K., and Revel, J. P. (1987) *Nature* **329**, 732-734
 52. Zhang, J.-T., and Nicholson, B. J. (1989) *J. Cell Biol.* **109**, 3391-3401
 53. Sosinsky, G. E. (1995) *Proc. Natl. Acad. Sci. U. S. A.* **92**, 9210-9214
 54. Kuraoka, A., Iida, H., Hatae, T., Shibata, Y., Itoh, M., and Kurita, T. (1993) *J. Histochem. Cytochem.* **41**, 971-980
 55. Kordel, M., Nicholson, B. J., and Harris, A. L. (1993) *Biophys. J.* **54**, A192 (abstr.)
 56. Davies, G. E., and Stark, G. R. (1970) *Proc. Natl. Acad. Sci. U. S. A.* **66**, 651-656
 57. Soumarmon, A., Robert, J. C., and Lewin, M. J. M. (1986) *Biochim. Biophys. Acta* **860**, 109-117
 58. Milligan, D. L., and Koshland, D. E., Jr. (1988) *J. Biol. Chem.* **263**, 6268-6275
 59. Wilcox, M. D., McKenzie, M. O., Parce, J. W., and Lyles, D. S. (1992) *Biochemistry* **31**, 10458-10464
 60. French, A. D., Murphy, V. G., and Kainuma, K. (1978) *J. Jap. Soc. Starch Sci.* **25**, 171-176
 61. French, A. D. (1979) *Bakers Digest* **53**, 39-46
 62. Jeffrey, G. A., and French, A. D. (1978) in *Molecular Structure by Diffraction Methods* (Sutton, E., and Treutter, M. R., eds) pp. 183-223, American Chemical Society, New York
 63. Hennemann, H., Kozjek, G., Dahl, E., Nicholson, B. J., and Willecke, K. (1992) *Eur. J. Cell Biol.* **58**, 81-89
 64. Risek, B., Klier, F. G., Phillips, A., Hahn, D. W., and Gilula, N. B. (1995) *J. Cell Sci.* **108**, 1017-1032
 65. Jiang, J. X., and Goodenough, D. A. (1996) *Proc. Natl. Acad. Sci. U. S. A.* **93**, 1287-1291
 66. Chen, Y. H., and DeHaan, R. L. (1996) *Am. J. Physiol.* **39**, C276-C285
 67. Stauffer, K. A. (1995) *J. Biol. Chem.* **270**, 6768-6772
 68. Ghosh, S., Safarik, R., Klier, G., Monosov, E., Gilula, N. B., and Kumar, N. M. (1995) *Mol. Biol. Cell* **6**, 189A (abstr.)
 69. Brink, P. R., Cronin, K., Banach, K., Peterson, E., Westphale, E. M., Seul, K. H., Ramanan, S. V., and Beyer, E. C. (1997) *Am. J. Physiol.*, **42**, C1386-C1396
 70. Baker, T. S., Caspar, D. L. D., Hollingshead, C. J., Goodenough, D. A., and Caspar, D. L. (1983) *J. Cell Biol.* **96**, 204-216
 71. Unger, V. M., Kumar, N. M., Gilula, N. B., and Yeager, M. (1997) *Nature Struct. Biol.* **4**, 39-43
 72. Perkins, G., Goodenough, D., and Sosinsky, G. (1997) *Biophys. J.* **72**, 533-544
 73. Downer, N. W. (1985) *Biophys. J.* **47**, 285-293
 74. Hoger, J. H., and Kaplan, S. (1985) *J. Biol. Chem.* **260**, 6932-6937
 75. Ludwig, F. R., and Jay, F. A. (1985) *Eur. J. Biochem.* **151**, 83-87
 76. Makowski, L., Caspar, D. L. D., Phillips, W. C., and Goodenough, D. A. (1984) *J. Mol. Biol.* **174**, 449-481
 77. Staros, J. V., and Anjaneyulu, P. S. R. (1989) *Methods Enzymol.* **172**, 609-628
 78. White, T. W., and Bruzzone, R. (1996) *J. Bioenerg. Biomembr.* **28**, 339-350
 79. Bukauskas, F. F., Elfgang, C., Willecke, K., and Weingart, R. (1995) *Pflügers Arch.* **429**, 870-872
 80. Kwak, B. R., Hermans, M. M. P., deJonge, H. R., Lohmann, S. M., Jongma, H. J., and Chanson, M. (1995) *Mol. Biol. Cell* **6**, 1707-1719
 81. Zambrowicz, E. B., and Colombini, M. (1993) *Biophys. J.* **65**, 1093-1100
 82. Suchyna, T. M., Veenstra, R. D., Chilton, M. G., and Nicholson, B. J. (1994) *Mol. Biol. Cell* **5S**, 199A (abstr.)
 83. Cao, F., Eckert, R., Elfgang, C., Hulser, D. F., Willecke, K., and Nicholson, B. J. (1994) *Mol. Biol. Cell* **5**, 198A (abstr.)
 84. Bevans, C., Brutyan, R. A., DeMaria, C., and Harris, A. L. (1995) *Biophys. J.* **68**, A204 (abstr.)
 85. Bevans, C. G., and Harris, A. L. (1995) *Mol. Biol. Cell* **6S**, 190A (abstr.)
 86. Zhou, X. W., Pfahnl, A., Werner, R., Hudder, A., Llanes, A., Luebke, A., and Dahl, G. (1997) *Biophys. J.* **72**, 1946-1953
 87. Oh, S., Bennett, M. V. L., Trexler, E. B., Verselis, V. K., and Bargiello, T. A. (1997) *Neuron* **19**, 927-938
 88. Buehler, L. K., Stauffer, K. A., Gilula, N. B., and Kumar, N. M. (1995) *Biophys. J.* **68**, 1767-1775
 89. Lawrence, T. S., Beers, W. H., and Gilula, N. B. (1978) *Nature* **272**, 501-506
 90. Murray, S. A., and Fletcher, W. H. (1984) *J. Cell Biol.* **98**, 1710-1719
 91. Piccolino, M., Neyton, J., and Gerschenfeld, H. M. (1984) *J. Neurosci.* **4**, 2477-2488
 92. Neveu, M. J., Hully, J. R., Babcock, K. L., Hertzberg, E. L., Nicholson, B. J., Paul, D. L., and Pitot, H. C. (1994) *J. Cell Sci.* **107**, 83-95
 93. Neveu, M. J., Sattler, C. A., Sattler, G. L., Hully, J. R., Hertzberg, E. L., Paul, D. L., Nicholson, B. J., and Pitot, H. C. (1994) *Mol. Carcin.* **11**, 145-154
 94. Janssen-Timmen, U., Traub, O., Dermietzel, R., Rabes, H. M., and Willecke, K. (1986) *Carcinogenesis* **7**, 1475-1482
 95. Eghbali, B., Kessler, J. A., Reid, L. M., Roy, C., and Spray, D. C. (1991) *Proc. Natl. Acad. Sci. U. S. A.* **88**, 10701-10705
 96. Gingalewski, C., Wang, K., Clemens, M. G., and Demiao, A. (1996) *J. Cell Physiol.* **166**, 461-467
 97. Mesnil, M., Krutovskikh, V. A., Piccoli, C., Elfgang, C., Traub, O., Willecke, K., and Yamasaki, H. (1995) *Cancer Res.* **55**, 629-639
 98. Bergoffen, J., Scherer, S. S., Wang, S., Scott, M. O., Bone, L. J., Paul, D. L., Chen, K., Lensch, M. W., Chance, P. F., and Fischbeck, K. H. (1993) *Science* **262**, 2039-2042